Published in final edited form as:
Neuron. 2012 January 12; 73(1): 121–134. doi:10.1016/j.neuron.2011.10.034.

Vti1a identifies a vesicle pool that preferentially recycles at rest and maintains spontaneous neurotransmission

Denise M.O. Ramirez[1], **Mikhail Khvotchev**[1], **Brent Trauterman**[1], and **Ege T. Kavalali**[1,2]

[1]Department of Neuroscience, UT Southwestern Medical Center, Dallas, TX 75390-9111, USA

[2]Department of Physiology, UT Southwestern Medical Center, Dallas, TX 75390-9111, USA

Summary

Recent studies suggest that synaptic vesicles (SVs) giving rise to spontaneous neurotransmission are distinct from those that carry out evoked release. However, the molecular basis of this dichotomy remains unclear. Here, we focused on two non-canonical SNARE molecules, Vps10p-tail-interactor-1a (vti1a) and VAMP7, previously shown to reside on SVs. Using simultaneous multicolor imaging at individual synapses, we could show that compared to the more abundant vesicular SNARE synaptobrevin, both vti1a and VAMP7 were reluctantly mobilized during activity. Vti1a, but not VAMP7, showed robust trafficking under resting conditions which could be partly matched by synaptobrevin. Furthermore, loss of vti1a function selectively reduced high frequency spontaneous neurotransmitter release detected postsynaptically. Expression of a truncated version of vti1a augmented spontaneous release more than full-length vti1a, suggesting an autoinhibitory process regulates vti1a function. Taken together, these results support the premise that in its native form vti1a selectively maintains spontaneous neurotransmitter release.

Introduction

Spontaneous neurotransmitter release is a salient feature of all presynaptic nerve terminals (Fatt and Katz, 1952). Recent studies have shown that these action potential (AP) independent release events are essential regulators of synaptic homeostasis in terms of both presynaptic release rate and postsynaptic sensitivity (Aoto et al., 2008; Frank et al., 2006; Lee et al., 2010; Sutton et al., 2006; Sutton et al., 2007). Moreover, there is growing evidence that postsynaptic receptors and signaling elements that respond to spontaneous release events diverge from those that respond to evoked release (Atasoy et al., 2008; Sara et al., 2011; Sutton et al., 2007), suggesting a spatial segregation of the two forms of neurotransmission (Zenisek, 2008). Furthermore, a number of studies have provided evidence that presynaptic vesicle populations giving rise to spontaneous release are distinct from those that carry out AP driven neurotransmission (Chung et al., 2010; Fredj and Burrone, 2009; Mathew et al., 2008; Sara et al., 2005; Virmani et al., 2005). However, this notion remains controversial as some studies have provided contradictory results (Groemer and Klingauf, 2007; Hua et al., 2010; Wilhelm et al., 2010). In the absence of molecular tags that identify a functionally distinct subpopulation of synaptic vesicles, it is difficult to

Correspondence should be addressed to: Ege T. Kavalali, Ph.D., Department of Neuroscience, U.T Southwestern Medical Center, 5323 Harry Hines Blvd., Dallas, TX 75390-9111, Phone: 214-648-1682, Fax: 214-648-1801, Ege.Kavalali@UTSouthwestern.edu.

ascertain whether these observations disagree in substance, or are merely due to vagaries of distinct experimental settings (Chung et al., 2010; Groemer and Klingauf, 2007; Prange and Murphy, 1999; Sara et al., 2005). Lack of molecular insight into this putative functional heterogeneity also renders the examination of specific signaling consequences of spontaneous release independent of other forms of neurotransmission difficult (Kavalali et al., 2011; Ramirez and Kavalali, 2011).

Synaptobrevin2 (syb2), a key vesicular SNARE essential for all forms of neurotransmission in the CNS, is widely distributed among all vesicle pools as its absence gives rise to deficits in evoked and spontaneous neurotransmission (Schoch et al., 2001). However, in contrast to the nearly complete ablation of Ca^{2+}-dependent evoked release, some spontaneous neurotransmission as well as other forms of release remain intact after loss of syb2, suggesting a role of alternative non-canonical vesicular SNAREs in the maintenance of certain forms of neurotransmission (Bhattacharya et al., 2002; Deitcher et al., 1998; Hua et al., 1998; Schoch et al., 2001). Several other SNAREs with a domain structure similar to that of syb2 are expressed at low levels on SVs, including VAMP4, VAMP7 and vti1a (Antonin et al., 2000b; Muzerelle et al., 2003; Scheuber et al., 2006; Takamori et al., 2006). Non-canonical SNAREs represent an attractive possibility to mediate specific forms of neurotransmission; indeed, recent studies implicate VAMP7 in the regulation of asynchronous and spontaneous release at the mossy fiber terminals (Scheuber et al., 2006). Additionally, the secretagogue α-latrotoxin can augment resting levels of release without relying on the canonical SNARE machinery components, implying that a separate complement of molecules may support spontaneous transmission (Deak et al., 2009).

Vti1a is a mammalian homolog of the yeast Q-SNARE vti1p, which is involved in transport between the endosome and the trans-Golgi network (Fischer von Mollard and Stevens, 1998). In neurons, vti1a is localized to cell bodies as well as presynaptic terminals, and a splice variant of this protein is enriched in purified SVs (Antonin et al., 2000b; Takamori et al., 2006). Although vti1a is not present in complex with the other classical SNAREs mediating SV fusion (syb2, SNAP-25, and syntaxin-1), it was shown to participate as a Qb-SNARE in complex with VAMP4, syntaxin-6, and syntaxin-13 (Antonin et al., 2000b; Kreykenbohm et al., 2002). Vti1a has been shown to participate in the recycling of SVs (Hoopmann et al., 2010), however, little is known of its role in synaptic transmission.

VAMP7, also known as tetanus toxin-insensitive VAMP (TI-VAMP), is a member of the longin subfamily of R-SNAREs. It is present predominantly in the Golgi apparatus, endosomes and lysosomes (Advani et al., 1998). In developing neurons, VAMP7 is localized to growth cones and regulates neurite outgrowth (Martinez-Arca et al., 2000). VAMP7 is expressed throughout the adult brain, typically in somatodendritic compartments, but is found in presynaptic terminals, most notably in hippocampal dentate granule cells (Muzerelle et al., 2003).

In this study, we focused on vti1a and VAMP7 and found that although both SNAREs are refractory to rapid mobilization during evoked stimulation, vti1a preferentially traffics under resting conditions. Further experiments showed that gain- and loss-of-function of vti1a results in up- and down-regulation of spontaneous event frequency, respectively. Our results support the notion that vti1a selectively maintains spontaneous neurotransmitter release in its native form.

Results

The distribution and trafficking of pHluorin-tagged VAMP7 and vti1a in hippocampal neurons

The lentiviral constructs encoding pHluorin-tagged syb2, vti1a and VAMP7 used in these studies are depicted in Figure 1A. Attachment of the pHluorin moiety at the SNARE C-terminus allows for visualization of SV trafficking because vesicular exocytosis results in pHluorin dequenching upon exposure to extracellular milieu (Miesenbock et al., 1998). Work from our laboratory has previously demonstrated that attachment of a GFP analog to the C-terminus of syb2 does not affect its function (Deak et al., 2006).

We confirmed the presynaptic vesicle localization of native vti1a and vti1a-pHluorin by immuno-electron microscopy (Figure 1B). The relative distributions of pHluorin-tagged vti1a and VAMP7 on the cell surface and in internal compartments were assessed by modification of external and internal pH and compared to the distribution of the pHluorin-tagged version of syb2 (synaptopHluorin). Figure 1C shows traces from experiments where we quantified changes in synaptic fluorescence relative to baseline (at pH 7.4) after bath application of pH 4 external solution and NH_4Cl. Syb2-pHluorin shows significant fluorescence at the surface and in internal compartments, consistent with earlier reports (Wienisch and Klingauf, 2006). Vti1a-pHluorin shows a similar distribution, suggesting this protein may also engage in synaptic vesicle recycling. VAMP7-pHluorin was expressed at lower levels in synaptic boutons compared to the other proteins examined, as evidenced by ~10 fold lower raw fluorescence intensity values after NH_4Cl application. VAMP7-pHluorin is predominantly expressed in internal compartments as shown by a relatively larger fluorescence change in response to NH_4Cl application compared to pH 4 external solution. Figure 1D depicts average data from multiple experiments.

We next examined the abilities of pHluorin-tagged syb2, vti1a and VAMP7 to undergo activity-dependent trafficking. As shown in Figure 1E, 400 APs given at 20 Hz to neurons expressing syb2-pHluorin elicited a substantial increase in fluorescence coincident with SV exocytosis. The same stimulation produced little increase in fluorescence in neurons expressing pHluorin-tagged vti1a or VAMP7, suggesting SVs containing these proteins show limited exocytosis in response to 20 Hz stimulation. In Figure 1F, the rising slopes of the fluorescence signal during 20 Hz stimulation were quantified from multiple independent experiments. Figure 1G shows average normalized peak fluorescence data. Approximately 20% of the total syb2-pHluorin molecules were exocytosed in response to 20 Hz stimulation, whereas about 5% of vti1a- or VAMP7-pHluorin molecules were exocytosed in response to the same stimulation. These results suggest that a large fraction of vti1a and VAMP7 reside in a resting pool, and that the vesicles containing the small proportion of vti1a and VAMP7 that exocytose in response to activity do so with significantly slower kinetics than syb2-pHluorin. These results agree with a recent study which demonstrated that a fraction of vti1a traffics on SVs as opposed to endosomes (Hoopmann et al., 2010).

The contribution of endocytosis to vti1a-pHluorin trafficking during 20 Hz stimulation was assessed by measuring fluorescence changes in the same synapses before and after treatment with the vacuolar ATPase inhibitor, folimycin. This compound prevents re-acidification of endocytosed vesicles (Drose and Altendorf, 1997) and therefore permits continued visualization of fused vesicles. We found that vti1a does not participate in rapid SV endocytosis during stimulation, because folimycin treatment did not reveal any increase in vti1a-pHluorin fluorescence compared to the same synapses imaged prior to treatment (Figure S1).

Vti1a preferentially traffics at rest

Next, we measured trafficking of vesicles containing pHluorin-tagged syb2, vti1a, or VAMP7 during both spontaneous and evoked transmission using folimycin. Treatment with this compound allows the small cumulative increases in fluorescence due to spontaneous transmission or mild evoked stimulation to be detected (Atasoy et al., 2008). As shown in Figure 2A, in 2 mM external Ca^{2+}, syb2- and VAMP7-pHluorin fluorescence signals increased minimally at rest, indicating that these proteins show only modest levels of spontaneous trafficking. These data are consistent with previous work showing syb2 mediates a portion of spontaneous release (Schoch et al., 2001). In contrast to its insensitivity to folimycin treatment during stimulation, vti1a exhibited a substantial fluorescence increase at rest, suggesting spontaneously released vesicles contain abundant vti1a. After 10 min. of imaging at rest, the neurons were subjected to 300 APs at 1 Hz in the same external solution. As expected, the rate of syb2 fluorescence change increased dramatically due to the stimulation-dependent exocytosis of syb2 containing vesicles. In contrast, the slope of fluorescence increase for vti1a decreased slightly during stimulation compared to the measurements at rest, whereas the slope for VAMP7 increased only slightly, suggesting little evoked release of vesicles containing vti1a and/or VAMP7. The slope of fluorescence increase at rest for vti1a is significantly higher than that of syb2, whereas the slope during 1Hz stimulation for syb2 is significantly higher than that of vti1a (Figure 2B). These results confirm that little vti1a is trafficked during evoked transmission, and suggest that vti1a is preferentially trafficked at rest. While these experiments utilized a full-length pHluorin-tagged version of vti1a, a longer alternative splice variant of the protein, designated vti1a-β, is reportedly enriched in synaptic terminals (Antonin et al., 2000b). We confirmed the subcellular localization and trafficking behaviors of vti1a-β at rest and with stimulation and found no differences between vti1a-β and full-length vti1a (Figure S2). Spontaneous trafficking of vti1a was also observed under similar conditions in the presence of tetrodotoxin (TTX) to block APs (Figure S3). Only small amounts of VAMP7 are mobilized during either spontaneous or evoked transmission.

Next, we repeated this experiment in 8 mM external Ca^{2+} to augment the rate of spontaneous transmission (Atasoy et al., 2008) and investigate possible Ca^{2+} regulation of vti1a-mediated spontaneous transmission. In the presence of elevated extracellular Ca^{2+}, syb2 trafficking was increased during both spontaneous and evoked transmission. Again, although the rate of the fluorescence increase for vti1a at rest is similar to those of syb2, the rate for vti1a during stimulation is slower than that of syb2 (Figure 2D–F). This result could indicate Ca^{2+}-sensitivity of vti1a trafficking at rest and confirms the relative lack of vti1a trafficking during evoked transmission.

Simultaneous dual color imaging of vesicular SNARE dynamics at individual synaptic boutons

In order to assess the trafficking behaviors of syb2 and vti1a or VAMP7 in the same boutons, we performed experiments using a dual-color confocal imaging technique. Figure S4A depicts a diagram of the construct encoding syb2 tagged with a pH-sensitive variant of dsRed, mOrange (Shaner et al., 2004). Panels S4B-M show images of neurons expressing both syb2-mOrange and pHluorin-tagged syb2, VAMP7 or vti1a after NH_4Cl treatment as well as intensity plots for each image. Syb2-mOrange co-localized in synaptic boutons (white arrows, Panels S4D, H, and L) with syb2-, VAMP7-, and vti1a-pHluorin as indicated by Pearson correlation values greater than 0.5.

We monitored the simultaneous trafficking of syb2 and vti1a or VAMP7 in the same boutons by co-expressing syb2-mOrange and pHluorin-tagged vti1a or VAMP7. The results of typical experiments are shown in Figure 3A–C. The increased fluorescence of syb2-

mOrange upon 20 Hz stimulation represents approximately 30% of the total syb2-mOrange present in the boutons examined. In the same boutons, about 10% of the total vti1a-pHluorin molecules and 20% of the total VAMP7-pHluorin molecules exhibited increased fluorescence upon stimulation. These results are consistent with the previous experiments (Figure 1D–F) and imply that SVs containing vti1a and syb2 are found in the same bouton but represent separate vesicle pools. Furthermore, these experiments provide additional evidence that vesicles containing vti1a are refractory to stimulation-dependent exocytosis. Data from multiple experiments are quantified in Figure 3D.

Next, we imaged neurons expressing syb2-mOrange and vti1a-pHluorin in external solution containing 2 or 8 mM $CaCl_2$ and folimycin at rest and during a 90 mM KCl stimulation. The results of typical experiments are shown in Figures 4A (2 mM $CaCl_2$) and 4D (8 mM $CaCl_2$). Similar to previous experiments (Figure 2), vesicles containing both syb2 and vti1a exhibited substantial fusion at rest. Further increases in syb2 fluorescence were seen during the 90 mM KCl treatment, indicative of evoked release, but were minimal in the case of vti1a at the same synapses. These results are quantified in the presence of 2 mM $CaCl_2$ and 8 mM $CaCl_2$ (Figure 4B, E). The inset depicts a sample graph indicating where the slope values were calculated. The differences between syb2 and vti1a slope values during chemical stimulation are significant in both 2 mM and 8 mM extracellular Ca^{2+}. Figures 4C and 4F depict the cumulative data as a percent of total internal fluorescence after NH_4Cl application. The inset depicts a sample graph indicating how the changes in fluorescence were calculated. The percentage of vti1a residing in internal compartments released during 90 mM K^+ stimulation is significantly less than that of syb2 in both 2 mM and 8 mM $CaCl_2$. The percentage of vti1a molecules that are trafficked at rest is significantly more than syb2 in the presence of 2 mM extracellular Ca^{2+}, but the spontaneous trafficking of syb2 and vti1a are approximately equal in the presence of elevated extracellular Ca^{2+}, corroborating earlier results (Figure 2). These results show that the majority of vti1a trafficking occurs at rest, and even with strong elevated K^+ stimulation, vti1a containing vesicles are released at a lower rate compared to those containing syb2. Furthermore, the simultaneous visualization of syb2 and vti1a trafficking during the 90 mM K^+ stimulation strongly suggests these proteins largely reside in different vesicular pools. We next assessed the simultaneous trafficking of VAMP7-pHluorin and syb2-mOrange. In experiments like those described for vti1a, syb2-mOrange was expressed in the same neurons as VAMP7-pHluorin and their spontaneous and evoked trafficking was measured simultaneously. Syb2-mOrange trafficked robustly both at rest and with 90 mM K^+ stimulation, but significantly less VAMP7 trafficking was observed under either condition (Figure S5). These results are comparable to earlier findings (Figure 2). While we did not observe robust mobilization of VAMP7-pHluorin either at rest or with stimulation, in contrast to Hua and colleagues (Hua et al., 2011), this is likely a result of the autoinhibitory actions of the longin domain, which was present in our full-length VAMP7 construct. Still, a measurable amount of VAMP7-pHluorin trafficking was seen in the same synapses as syb2-mOrange, which agrees well with the basic finding of their report that VAMP7 is targeted to a subpool of SVs.

In light of recent work showing a role of endosomal sorting in SV recycling (Hoopmann et al., 2010), we evaluated the overlap between the trafficking behaviors of vti1a and two *bona fide* endosomal markers, transferrin receptor (TfR) (Kennedy et al., 2010) and syntaxin-6 (Rizzoli et al., 2006) (Figure S6). TfR and syntaxin-6 showed limited spontaneous trafficking in synapses compared to vti1a. Thus, although vti1a resides in endosomes (Antonin et al., 2000a; Bethani et al., 2009; Kunwar et al., 2011) in addition to its presence on SVs (Antonin et al., 2000b; Takamori et al., 2006), endosomal fusion seems unlikely to contribute to the fluorescence increases seen at rest with vti1a-pHluorin or -mOrange, supporting the notion that vti1a functions in the spontaneous release of *bona fide* SVs.

Endogenous levels of vti1a correlate with the degree of spontaneous vesicle recycling detected at individual presynaptic terminals

To visualize spontaneously recycling SVs, we labeled live neurons with anti-synaptotagmin-1 (syt1) lumenal domain antibodies in the presence of TTX then immunostained for endogenous vti1a (Figure 4G). Representative images and an intensity plot are shown in Figures 4H–K. In the merged image, many vti1a-positive puncta colocalized with lumenal syt1 staining as shown by the white arrows. We found a strong positive correlation between the intensity of syt1 staining and native vti1a staining (mean Pearson correlation = 0.66 ± 0.02 from 14 images). This finding confirms that native vti1a is localized to spontaneously recycling SVs, as indicated by our previous experiments utilizing vti1a-pHluorin. Furthermore, we were able to visualize both the native and pHluorin-tagged versions of vti1a at the ultrastructural level within presynaptic terminals, in a pattern consistent with a vesicular localization (Figures 1, S7). Both endogenous vti1a and vti1a-pHluorin were associated with vesicular structures with an average diameter of 35–40 nm, consistent with the reported diameter of synaptic vesicles (Harris and Sultan, 1995). Together, these immunostaining data confirm the presence of vti1a on SVs (Antonin et al., 2000b; Takamori et al., 2006), establish the validity of studying trafficking behaviors of the pHluorin-tagged version of vti1a, and further support the notion that vti1a traffics at rest.

Knockdown of vti1a selectively impairs spontaneous neurotransmission

The experiments presented so far describe the novel trafficking behaviors of vti1a, in which vesicles containing this protein are specifically mobilized at rest, presumably during spontaneous neurotransmission, but only reluctantly during a variety of evoked stimulation paradigms. As a first step to validate this premise, miniature (mIPSCs) and evoked inhibitory postsynaptic currents were recorded from neurons in which the expression of vti1a was knocked down. Figure 5A depicts a schematic of the short hairpin RNA (shRNA) construct used to knock down vti1a. A representative immunoblot of neuronal protein samples harvested from cells expressing shRNAs directed against vti1a (vti1a-1 KD and vti1a-3 KD) is shown in Figure 5B. Both shRNAs effect a substantial knockdown of vti1a protein levels. Reduced levels of vti1a do not cause compensatory changes in expression of the closely related protein, vti1b. Evoked inhibitory responses were measured from neurons expressing vti1a-1 KD, vti1a-3 KD, and L307. Figure 5C depicts representative traces from a stimulation train consisting of 50 APs given at 10 Hz. Average amplitudes for each response in the train are shown in Figure 5D. The inset shows paired-pulse ratios from the same recordings. No differences were seen in the peak amplitudes or paired-pulse ratios among neurons expressing L307, vti1a-1 KD, or vti1a-3 KD, showing that vti1a does not affect evoked inhibitory release. Next, mIPSCs were recorded from neurons expressing vti1a-1 KD, vti1a-3 KD, and L307. Representative mIPSC traces are shown in Figure 5E. Cumulative probability histograms of mIPSC inter-event intervals are shown in Figure 5F. Vti1a knockdown selectively impairs high-frequency spontaneous transmission at low inter-event intervals, as shown by lower cumulative probabilities in recordings from neurons infected with vti1a-1 KD and vti1a-3 KD compared to L307-infected neurons. The decrease in mIPSC frequency detected after vti1a knockdown can be completely rescued by co-expression of vti1a-pHluorin (Figure S8). Finally, mEPSCs were recorded from neurons expressing vti1a-1 KD, vti1a-3 KD and L307 (Figure 5G). Similar to the results seen in measurements of spontaneous inhibitory transmission, a reduction in the cumulative probability of high-frequency spontaneous excitatory events is observed in neurons in which vti1a expression is reduced (Figure 5H). Neither mIPSC nor mEPSC amplitudes recorded from neurons expressing vti1a-1 KD or vti1a-3 KD were significantly different from L307-infected neurons (mIPSC: L307=29.9 ± 3.5 pA, vti1a-1 KD=38.2 ± 2.8 pA, p=0.07, vti1a-3 KD=21.8 ± 2.5 pA, p=0.08; mEPSC L307=32.9 ± 3.7 pA, vti1a-1 KD=26.8 ± 2.5 pA, p=0.21, vti1a-3 KD= 26.7 ± 5 pA, p=0.38). Collectively, these results reveal a specific role

for vti1a in spontaneous transmission, corroborating the optical imaging results described above.

Expression of a truncated version of vti1a augments spontaneous release

To investigate whether vti1a could exert a gain-of-function effect on spontaneous release rate detected postsynaptically, we next assessed the effect of expression of vti1a-pHluorin and a pHluorin-tagged mutant protein lacking the N-terminal region before the SNARE motif, ΔN vti1a, on spontaneous transmission. We chose to study this mutant vti1a due to this protein's domain homology to VAMP7 and other longins, whose N-termini are known to negatively regulate SNARE complex formation (Pryor et al., 2008; Tochio et al., 2001). A schematic diagram of the ΔN vti1a-pHluorin protein structure is shown in Figure 6A. As with full-length vti1a-pHluorin (Figures S4J–M), ΔN vti1a-pHluorin colocalizes with syb2-mOrange in punctate structures reminiscent of synaptic terminals (Figures 6B–6E). We characterized the subcellular localization and trafficking behaviors of the ΔN vti1a-pHluorin mutant using bath application of acidified and NH_4Cl-containing extracellular solution as in Figure 1B (Figure 6F, G). Deletion of the N-terminal portion of vti1a shifts the distribution of the mutant protein towards the surface. ΔN vti1a-pHluorin exhibits trafficking behavior during spontaneous and evoked transmission similar to that of full-length vti1a (Figures 6H and 6I, see also 2A and 2B). An increase in ΔN vti1a-pHluorin fluorescence was seen at rest in the presence of 2 mM $CaCl_2$ and folimycin, but no further increase was seen upon 1 Hz stimulation. A small increase in fluorescence was seen after NH_4Cl treatment, representative of ΔN vti1a-pHluorin residing in internal compartments. We next recorded mIPSCs from uninfected neurons or neurons expressing full-length vti1a- or ΔN vti1a-pHluorin. Representative traces are shown in Figure 6J and cumulative probability histograms of the inter-event intervals are shown in Figure 6K. Significant increases were seen in mIPSC frequency in neurons expressing either wild-type or ΔN vti1a-pHluorin, and this difference was greatest at low inter-event intervals, consistent with the results of the vti1a knockdown studies (Figure 5E–H). The effect of ΔN vti1a-pHluorin expression was greater than that of the wild-type protein, consistent with the notion of an autoinhibitory function of the N-terminal portion of vti1a. No significant differences were seen in average mIPSC amplitude between wild-type neurons and those expressing vti1a- or ΔN vti1a-pHluorin (wild-type = 37.8 ± 5.3 pA, vti1a = 40.1 ± 3.3 pA, p=0.72, ΔN vti1a= 38 ± 3.8 pA, p=0.98). Similar results were seen with spontaneous excitatory transmission. Sample traces of recordings from uninfected neurons or neurons expressing full-length vti1a- or ΔN vti1a-pHluorin are shown in Figure 6L. Cumulative probability histograms of the inter-event intervals are shown in Figure 6M. Although expression of full-length vti1a has little effect on mEPSC frequency, expression of ΔN vti1a-pHluorin robustly increases the probability of high-frequency spontaneous events. Differences seen in average mEPSC amplitudes between wild-type neurons and those expressing vti1a- or ΔN vti1a-pHluorin were significant (wild-type = 25.6 ± 1.4 pA, vti1a = 20.2 ± 0.9 pA, p=0.005, ΔN vti1a= 35.06 ± 3.9 pA, p=0.03) suggesting a potential postsynaptic effect of vti1a or a possible consequence of alterations in spontaneous glutamate release. These data complement the loss-of-function studies described above and support a specific role for vti1a in meditating spontaneous transmission. Additionally, the data suggest an autoinhibitory function for the N-terminus of vti1a.

Spontaneous trafficking of vti1a persists in the absence of syb2

Our current data suggest a specific role for vti1a in spontaneous neurotransmission, as well as the presence of this SNARE on a pool of vesicles distinct from those containing syb2. To address whether vti1a traffics independently of syb2, we monitored the spontaneous trafficking of vti1a-pHluorin in syb2 knockout (KO) neurons. As a control, syb2-pHluorin trafficking was monitored in separate cultures of syb2 KO neurons. An averaged time course

from multiple experiments is shown in Figure 7A. No differences were found between syb2- and vti1a-pHluorin trafficking in the average slope values of the increase in fluorescence at rest (Figure 7B) or the percent of total fluorescence generated during spontaneous activity normalized to the total protein levels visualized after NH_4Cl treatment (Figure 7C). These findings strongly argue that vti1a is localized to a pool of vesicles distinct from those containing syb2, which is mobilized at rest. Next, we measured mIPSCs in uninfected syb2 KO neurons or those expressing full-length or ΔN vti1a-pHluorin together with wild-type littermate control cultures. Sample traces are shown in Figure 7D, and frequency data from multiple recording are quantified in Figure 7E. As previously reported, syb2 KO neurons exhibit significantly decreased mIPSC frequency compared to littermate controls (Schoch et al., 2001). Vti1a-pHluorin expression has no effect on mIPSC frequency in syb2 KO neurons, whereas ΔN vti1a-pHluorin expression dramatically increases mIPSC frequency, similar to the results shown for wild-type neurons (Figures 6J, 6K). Next, we assessed the effect of vti1a knockdown in the absence of syb2. In Figure 7F, sample mIPSC traces of uninfected syb2 KO neurons or those infected with vti1a-1 KD or vti1a-3 KD are depicted. Although syb2 KO neurons exhibit reduced mIPSC frequency compared to wild-type neurons (see panel E), knockdown of vti1a essentially abolished the remaining spontaneous neurotransmission seen in these neurons. Cumulative histogram data from multiple recordings are presented in Figure 7G and show significantly decreased mIPSC frequency in syb2 KO/vti1a knockdown neurons compared to uninfected syb2 KO neurons. Vti1a knockdown did not affect average mIPSC amplitudes in the absence of syb2 (syb2 KO = 15.84 ± 1.57 pA, syb2 KO/vti1a-1 KD = 12.55 ± 0.99 pA, and syb2 KO/vti1a-3 KD = 16.22 ± 2.31 pA). While knockout of syb2 impairs most evoked synaptic vesicle trafficking (Schoch et al., 2001), we show that the functional impact of vti1a (as judged by fluorescence imaging as well as electrophysiology) is identical to its properties seen in wild-type synapses. These findings argue for a direct executive function of vti1a in spontaneous release that is independent of syb2.

Discussion

At central synapses, syb2 is the predominant vesicular SNARE that ensures rapid execution and fidelity of fusion reactions (Schoch et al., 2001). However, loss-of-function studies of syb2 as well as other key SNAREs involved in fusion suggest a parallel pathway, possibly involving non-canonical SNAREs typically implicated in constitutive vesicle trafficking, may mediate fusion and recycling of a subset of vesicles (Bronk et al., 2007; Deak et al., 2004; Schoch et al., 2001; Washbourne et al., 2002). Recent observations that vesicles giving rise to evoked and spontaneous neurotransmitter release may originate from distinct pools (Chung et al., 2010; Fredj and Burrone, 2009; Sara et al., 2005), taken together with the finding that this distinction is largely lost in syb2 deficient synapses (Sara et al., 2005), prompted us to survey non-canonical SNAREs shown to be resident on SVs (Takamori et al., 2006) that may selectively sustain spontaneous release.

Fluorescence imaging experiments revealed that both vti1a and VAMP7 were capable of trafficking at rest. Vti1a, however, possessed a more prominent intracellular pool and more robust trafficking at rest compared to VAMP7. These results are consistent with the subcellular localizations of syb2-, vti1a-, and VAMP7-pHluorin revealed by manipulation of intracellular and extracellular pH values (Figure 1) insofar as significant amounts of spontaneous vesicle trafficking are expected to drive the surface exposure of a larger fraction of synaptic vesicle proteins. Vesicles containing vti1a or VAMP7 showed relatively reluctant responses to AP evoked stimulation compared to swift mobilization of syb2-containing vesicles during evoked neurotransmission. These differences were more pronounced during elevated K+ induced depolarization, a strong stimulation paradigm that typically mobilizes all recycling pool vesicles in central synapses (Harata et al., 2001). A

key advantage of our fluorescence imaging approach was the use of dual color imaging, which enabled us to compare mobilization kinetics of vti1a and VAMP7 to the canonical trafficking of syb2 at individual synapses. Kinetic differences detected between syb2 and these non-canonical SNAREs are hard to reconcile with a single pool model and support the notion that these molecules largely reside in distinct populations of vesicles. Our findings are consistent with a recent report identifying the specific targeting of VAMP7 to the resting vesicular pool (Hua et al., 2011).

The trafficking properties of vti1a correspond well with several key features of the putative spontaneously recycling SV pool described in earlier studies (Sara et al., 2005). Vesicles containing vti1a robustly fuse in the absence of AP stimulation, but remain largely refractory to low frequency AP activity. However, these vesicles can be partly, albeit reluctantly, mobilized during higher frequency stimulation as well as elevated K^+ stimulation. Therefore, the molecularly specific analysis we present here suggests that spontaneously recycling SVs are not unresponsive to activity per se, but require higher intensities of stimulation and Ca^{2+} influx to trigger measurable synaptic responses. The properties of vesicle trafficking mediated by vti1a, therefore, also highly resemble the type of synaptic activity that can be detected in nascent synaptic terminals connecting immature neuronal populations (Mozhayeva et al., 2002).

At the cellular level, spontaneous release can be detected at a wide frequency spectrum. This broad range may reflect the higher spontaneous release probability of some synapses due to heterogeneities in spontaneous release machineries as well as fluctuations in intraterminal Ca^{2+} levels (Abenavoli et al., 2002; Llano et al., 2000; Xu et al., 2009). In our experiments, the decrease in vti1a levels via shRNA- mediated knock down had a strong impact on the high frequency, short inter-event interval component of release, which is consistent with the robust spontaneous trafficking of vti1a. Moreover, the impact of vtia1a on neurotransmission was detectable in both excitatory and inhibitory synapses.

Negative regulation of SNARE complex formation by intramolecular binding of the longin domain with the SNARE motif has been shown for the longin Ykt6 (Tochio et al., 2001), and suggested for VAMP7 (Pryor et al., 2008). In our experiments, expression of truncated vti1a triggered a prominent augmentation of baseline levels of spontaneous release detected electrophysiologically, suggesting the existence of a mechanism that may circumvent potential autoinhibition of vti1a, akin to earlier proposals of VAMP7 as well as syntaxin1 function (Dulubova et al., 1999; Pryor et al., 2008). Indeed, VAMP7-pHluorin lacking the longin domain has an increased rate of spontaneous exocytosis compared to full-length VAMP7 (Hua et al., 2011).

In earlier studies, individual knockouts of vti1a and vti1b did not reveal significant phenotypes, whereas the double knockout of these proteins triggered severe abnormalities in neuronal development (Atlashkin et al., 2003; Kunwar et al., 2011). Well-characterized roles of these proteins in constitutive endosomal trafficking may complicate the evaluation of their loss-of-function phenotypes with respect to their specific role in synaptic transmission. Nevertheless, the shRNA-based loss-of-function experiments showed a specific reduction in spontaneous release, indicating that shRNA-based knockdown of vti1a can provide insight into synaptic role(s) of vti1a without compromising neuronal survival. Typically, incomplete reductions in SNARE proteins do not result in discernable phenotypes as these proteins are present in excess quantities beyond minimum requirements (Bethani et al., 2009), therefore it is noteworthy that in our hands knockdown of vti1a gave rise to a distinct synaptic phenotype. This finding suggests that the amount of vti1a present on vesicles may encode a rate limiting step regulating levels of spontaneous release. At the level of the whole organism, a selective deficit in spontaneous neurotransmitter release may not give rise to an

overt phenotype. For instance, mice that lack double C2 domain 2b (doc2b) show a specific deficit in Ca^{2+}-dependent regulation of spontaneous release without overt alterations in behavior (Groffen et al., 2010; Pang et al., 2011). However, spontaneous release deficits in doc2b knockouts and those potentially associated with vti1a or vti1b single knockouts may lead to subtle changes in behavior which would require closer examination. Indeed, spontaneous neurotransmission has recently been shown to mediate the fast acting antidepressant action of NMDA receptor blockers on mouse behavior (Autry et al., 2011).

A growing number of studies suggest that spontaneous neurotransmitter release can be regulated independently of evoked neurotransmission (Ramirez and Kavalali, 2011). Identification of a distinct pool marked by vti1a should be taken as one factor contributing to a larger context of other observations, which together can explain why spontaneous and evoked SV trafficking processes are functionally segregated. The functional properties of key vesicular SNARE molecules we described here may provide an attractive substrate for signal transduction pathways triggering the differential regulation of spontaneous and evoked release. The differences in regulation of the two forms of release, therefore, may not only arise from their distinct Ca^{2+} dependence (Groffen et al., 2010; Xu et al., 2009) but also stem from their reliance on distinct release machineries nucleated by different vesicular SNAREs. Overall, the co-existence of molecularly distinct SV populations with different fusion properties may allow certain regulatory pathways to impact a particular type of neurotransmission selectively, thereby triggering a specific cellular response. Such relationships may be seen in cases where the nature of presynaptic activity can determine the impact of downstream signaling events (Atasoy et al., 2008; Kavalali et al., 2011; Sutton et al., 2007).

Experimental Procedures

Cell Culture

Dissociated hippocampal cultures from postnatal day 0–3 Sprague-Dawley rats or embryonic day 18 syb2-2 KO mice with their littermate controls were prepared as previously described (Kavalali et al., 1999; Schoch et al., 2001). All experiments were performed on 14–21 DIV cultures. (see Supplementary Materials for further details)

Lentiviral Preparation

We generated lentiviral expression constructs encoding the mouse versions of vti1a, an N-terminal truncation mutant of vti1a designated ΔN vti1a, and VAMP7 tagged at their C-termini by removing the syb2 coding sequence from a plasmid encoding synaptopHluorin (Miesenbock et al., 1998) and subcloning the desired coding sequences for these proteins in frame with the pHluorin sequence into the pFUGW vector (Lois et al., 2002). (see Supplementary Materials for further details)

Single Color Imaging

Neurons expressing pHluorin-tagged syb2, vti1a, ΔN vti1a, or VAMP7 were imaged on a Nikon TE2000-U inverted microscope using a Cascade 512 cooled CCD camera (Roper Scientific) and Metafluor 7.6 software (Molecular Dynamics). Experiments were performed in a modified Tyrode's solution containing (in mM): 150 NaCl, 4 KCl, 2 $MgCl_2$, 2 $CaCl_2$, 10 glucose, 10 HEPES, pH 7.4. The Tyrode's solution also contained the glutamate receptor blockers AP-5 (50 μM) and CNQX (10 μM) to prevent excitotoxicity. In all imaging experiments, 50 mM NH_4Cl treatment was used at the end of the experiment to estimate total protein expression. (see Supplementary Materials for further details)

Dual Color Imaging

Neurons co-expressing syb2-mOrange and either syb2-, vti1a-, or VAMP7-pHluorin were imaged in Tyrode's solution on a Zeiss LSM510 confocal microscope using LSM 5 software. (see Supplementary Materials for further details)

Immunocytochemistry

Neurons were incubated for 15 min. at room temperature with rabbit polyclonal antibodies against the lumenal epitope of syt1 (1:100 dilution, Synaptic Systems) in Tyrode's solution containing 1 μM TTX. The neurons were then processed for vti1a immunocytochemistry (using an anti-vti1a mouse monoclonal antibody, 1:200, BD Biosciences) as described (Ramirez et al., 2008). (see Supplementary Materials for further details)

Electrophysiology

Whole-cell patch-clamp recordings were performed on hippocampal pyramidal neurons as described (Nosyreva and Kavalali, 2010). (see Supplementary Materials for further details)

Western Blotting

Western blots to assess vti1a knockdown were performed as described in (Nosyreva et al 2010). The primary antibodies were: anti-vti1a mouse monoclonal at 1:500 dilution (BD Biosciences), anti-vti1b rabbit polyclonals at 1:500 dilution (Synaptic systems, Goettingen, Germany), and anti-Rab-GDI mouse monoclonal at 1:15000 dilution (gift of Dr. T. Südhof). Using vti1a-1 KD, the mean knockdown efficiency of vit1a was 94 ± 2.5% compared to L307-infected neurons. Using vti1a-3 KD, the mean knockdown efficiency of vti1a was 77.9 ± 4.7% compared to L307-infected neurons.

Immuno-electron Microscopy

Wild-type neurons or those infected with vti1a-pHluorin or vti1a-1 KD lentiviruses were fixed in 0.1% glutaraldehyde, 4% paraformaldehyde in PBS (pH 7.4), and examined by immunoelectron microscopy using a rabbit antibody to GFP or a mouse monoclonal antibody against vti1a (BD Biosciences) essentially as described (Virmani et al., 2003). Electron microscopy experiments were performed by the Molecular and Cellular Imaging Facility at UT Southwestern Medical Center. (see Supplementary Materials for further details)

Supplementary Material

Refer to Web version on PubMed Central for supplementary material.

Acknowledgments

This work is supported by grants from the NIMH (R01MH066198) to E.T.K and (F32MH093109) to D.M.O.R. We thank Dr. Thomas C. Südhof for his encouragement and support at the initial stages of this work. We thank Drs. Megumi Adachi and Pei Liu for assistance with syb2 knockout mice. We also thank Dr. Thierry Galli for the initial VAMP7 expression construct and Drs. Matthew Kennedy and Michael Ehlers for the TfR-pHluorin construct. We greatly appreciate Dr. Christopher Gilpin's help with immuno-EM analysis and Dr. Manjot Bal sharing syntaxin6 expressing neurons. We gratefully acknowledge Dr. Lisa M. Monteggia for discussions and her critical insight during this project.

References

Abenavoli A, Forti L, Bossi M, Bergamaschi A, Villa A, Malgaroli A. Multimodal quantal release at individual hippocampal synapses: evidence for no lateral inhibition. J Neurosci. 2002; 22:6336–6346. [PubMed: 12151511]

Advani RJ, Bae HR, Bock JB, Chao DS, Doung YC, Prekeris R, Yoo JS, Scheller RH. Seven novel mammalian SNARE proteins localize to distinct membrane compartments. J Biol Chem. 1998; 273:10317–10324. [PubMed: 9553086]

Antonin W, Holroyd C, Fasshauer D, Pabst S, Von Mollard GF, Jahn R. A SNARE complex mediating fusion of late endosomes defines conserved properties of SNARE structure and function. EMBO J. 2000a; 19:6453–6464. [PubMed: 11101518]

Antonin W, Riedel D, von Mollard GF. The SNARE Vti1a-beta is localized to small synaptic vesicles and participates in a novel SNARE complex. J Neurosci. 2000b; 20:5724–5732. [PubMed: 10908612]

Aoto J, Nam CI, Poon MM, Ting P, Chen L. Synaptic signaling by all-trans retinoic acid in homeostatic synaptic plasticity. Neuron. 2008; 60:308–320. [PubMed: 18957222]

Atasoy D, Ertunc M, Moulder KL, Blackwell J, Chung C, Su J, Kavalali ET. Spontaneous and evoked glutamate release activates two populations of NMDA receptors with limited overlap. J Neurosci. 2008; 28:10151–10166. [PubMed: 18829973]

Atlashkin V, Kreykenbohm V, Eskelinen EL, Wenzel D, Fayyazi A, Fischer von Mollard G. Deletion of the SNARE vti1b in mice results in the loss of a single SNARE partner, syntaxin 8. Molecular and cellular biology. 2003; 23:5198–5207. [PubMed: 12861006]

Autry AE, Adachi M, Nosyreva E, Na ES, Los MF, Cheng P-f, Kavalali ET, Monteggia LM. NMDA receptor blockade at rest triggers rapid behavioural antidepressant responses. Nature. 2011; 475:91–95. [PubMed: 21677641]

Bethani I, Werner A, Kadian C, Geumann U, Jahn R, Rizzoli SO. Endosomal fusion upon SNARE knockdown is maintained by residual SNARE activity and enhanced docking. Traffic (Copenhagen, Denmark). 2009; 10:1543–1559.

Bhattacharya S, Stewart BA, Niemeyer BA, Burgess RW, McCabe BD, Lin P, Boulianne G, O'Kane CJ, Schwarz TL. Members of the synaptobrevin/vesicle-associated membrane protein (VAMP) family in Drosophila are functionally interchangeable in vivo for neurotransmitter release and cell viability. Proc Natl Acad Sci U S A. 2002; 99:13867–13872. [PubMed: 12364587]

Bronk P, Deak F, Wilson MC, Liu X, Sudhof TC, Kavalali ET. Differential effects of SNAP-25 deletion on Ca2+-dependent and Ca2+-independent neurotransmission. J Neurophysiol. 2007; 98:794–806. [PubMed: 17553942]

Chung C, Barylko B, Leitz J, Liu X, Kavalali ET. Acute dynamin inhibition dissects synaptic vesicle recycling pathways that drive spontaneous and evoked neurotransmission. J Neurosci. 2010; 30:1363–1376. [PubMed: 20107062]

Deak F, Liu X, Khvotchev M, Li G, Kavalali ET, Sugita S, Sudhof TC. Alpha-latrotoxin stimulates a novel pathway of Ca2+-dependent synaptic exocytosis independent of the classical synaptic fusion machinery. J Neurosci. 2009; 29:8639–8648. [PubMed: 19587270]

Deak F, Schoch S, Liu X, Sudhof TC, Kavalali ET. Synaptobrevin is essential for fast synaptic-vesicle endocytosis. Nat Cell Biol. 2004; 6:1102–1108. [PubMed: 15475946]

Deak F, Shin OH, Kavalali ET, Sudhof TC. Structural determinants of synaptobrevin 2 function in synaptic vesicle fusion. J Neurosci. 2006; 26:6668–6676. [PubMed: 16793874]

Deitcher DL, Ueda A, Stewart BA, Burgess RW, Kidokoro Y, Schwarz TL. Distinct requirements for evoked and spontaneous release of neurotransmitter are revealed by mutations in the Drosophila gene neuronal-synaptobrevin. J Neurosci. 1998; 18:2028–2039. [PubMed: 9482790]

Drose S, Altendorf K. Bafilomycins and concanamycins as inhibitors of V-ATPases and P-ATPases. The Journal of experimental biology. 1997; 200:1–8. [PubMed: 9023991]

Dulubova I, Sugita S, Hill S, Hosaka M, Fernandez I, Sudhof TC, Rizo J. A conformational switch in syntaxin during exocytosis: role of munc18. Embo J. 1999; 18:4372–4382. [PubMed: 10449403]

Fatt P, Katz B. Spontaneous subthreshold activity at motor nerve endings. J Physiol. 1952; 117:109–128. [PubMed: 14946732]

Fischer von Mollard G, Stevens TH. A human homolog can functionally replace the yeast vesicle-associated SNARE Vti1p in two vesicle transport pathways. J Biol Chem. 1998; 273:2624–2630. [PubMed: 9446565]

Frank CA, Kennedy MJ, Goold CP, Marek KW, Davis GW. Mechanisms underlying the rapid induction and sustained expression of synaptic homeostasis. Neuron. 2006; 52:663–677. [PubMed: 17114050]

Fredj NB, Burrone J. A resting pool of vesicles is responsible for spontaneous vesicle fusion at the synapse. Nat Neurosci. 2009; 12:751–758. [PubMed: 19430474]

Groemer TW, Klingauf J. Synaptic vesicles recycling spontaneously and during activity belong to the same vesicle pool. Nat Neurosci. 2007; 10:145–147. [PubMed: 17220885]

Groffen AJ, Martens S, Diez Arazola R, Cornelisse LN, Lozovaya N, de Jong AP, Goriounova NA, Habets RL, Takai Y, Borst JG, et al. Doc2b is a high-affinity Ca2+ sensor for spontaneous neurotransmitter release. Science. 2010; 327:1614–1618. [PubMed: 20150444]

Harata N, Pyle JL, Aravanis AM, Mozhayeva M, Kavalali ET, Tsien RW. Limited numbers of recycling vesicles in small CNS nerve terminals: implications for neural signaling and vesicular cycling. Trends Neurosci. 2001; 24:637–643. [PubMed: 11672807]

Harris KM, Sultan P. Variation in the number, location and size of synaptic vesicles provides an anatomical basis for the nonuniform probability of release at hippocampal CA1 synapses. Neuropharmacology. 1995; 34:1387–1395. [PubMed: 8606788]

Hoopmann P, Punge A, Barysch SV, Westphal V, Buckers J, Opazo F, Bethani I, Lauterbach MA, Hell SW, Rizzoli SO. Endosomal sorting of readily releasable synaptic vesicles. Proc Natl Acad Sci U S A. 2010; 107:19055–19060. [PubMed: 20956291]

Hua SY, Raciborska DA, Trimble WS, Charlton MP. Different VAMP/synaptobrevin complexes for spontaneous and evoked transmitter release at the crayfish neuromuscular junction. J Neurophysiol. 1998; 80:3233–3246. [PubMed: 9862918]

Hua Y, Sinha R, Martineau M, Kahms M, Klingauf J. A common origin of synaptic vesicles undergoing evoked and spontaneous fusion. Nat Neurosci. 2010; 13:1451–1453. [PubMed: 21102448]

Hua Z, Leal-Ortiz S, Foss SM, Waites CL, Garner CC, Voglmaier SM, Edwards RH. v-SNARE Composition Distinguishes Synaptic Vesicle Pools. Neuron. 2011; 71:474–487. [PubMed: 21835344]

Kavalali ET, Chung C, Khvotchev M, Leitz J, Nosyreva E, Raingo J, Ramirez DM. Spontaneous neurotransmission: an independent pathway for neuronal signaling? Physiology (Bethesda, Md. 2011; 26:45–53.

Kavalali ET, Klingauf J, Tsien RW. Activity-dependent regulation of synaptic clustering in a hippocampal culture system. Proc Natl Acad Sci U S A. 1999; 96:12893–12900. [PubMed: 10536019]

Kennedy MJ, Davison IG, Robinson CG, Ehlers MD. Syntaxin-4 defines a domain for activity-dependent exocytosis in dendritic spines. Cell. 2010; 141:524–535. [PubMed: 20434989]

Kreykenbohm V, Wenzel D, Antonin W, Atlachkine V, von Mollard GF. The SNAREs vti1a and vti1b have distinct localization and SNARE complex partners. European journal of cell biology. 2002; 81:273–280. [PubMed: 12067063]

Kunwar AJ, Rickmann M, Backofen B, Browski SM, Rosenbusch J, Schoning S, Fleischmann T, Krieglstein K, Fischer von Mollard G. Lack of the endosomal SNAREs vti1a and vti1b led to significant impairments in neuronal development. Proc Natl Acad Sci U S A. 2011; 108:2575–2580. [PubMed: 21262811]

Lee MC, Yasuda R, Ehlers MD. Metaplasticity at single glutamatergic synapses. Neuron. 2010; 66:859–870. [PubMed: 20620872]

Llano I, Gonzalez J, Caputo C, Lai FA, Blayney LM, Tan YP, Marty A. Presynaptic calcium stores underlie large-amplitude miniature IPSCs and spontaneous calcium transients. Nat Neurosci. 2000; 3:1256–1265. [PubMed: 11100146]

Lois C, Hong EJ, Pease S, Brown EJ, Baltimore D. Germline transmission and tissue-specific expression of transgenes delivered by lentiviral vectors. Science. 2002; 295:868–872. [PubMed: 11786607]

Martinez-Arca S, Alberts P, Zahraoui A, Louvard D, Galli T. Role of tetanus neurotoxin insensitive vesicle-associated membrane protein (TI-VAMP) in vesicular transport mediating neurite outgrowth. J Cell Biol. 2000; 149:889–900. [PubMed: 10811829]

Mathew SS, Pozzo-Miller L, Hablitz JJ. Kainate modulates presynaptic GABA release from two vesicle pools. J Neurosci. 2008; 28:725–731. [PubMed: 18199771]

Miesenbock G, De Angelis DA, Rothman JE. Visualizing secretion and synaptic transmission with pH-sensitive green fluorescent proteins. Nature. 1998; 394:192–195. [PubMed: 9671304]

Mozhayeva MG, Sara Y, Liu X, Kavalali ET. Development of vesicle pools during maturation of hippocampal synapses. J Neurosci. 2002; 22:654–665. [PubMed: 11826095]

Muzerelle A, Alberts P, Martinez-Arca S, Jeannequin O, Lafaye P, Mazie JC, Galli T, Gaspar P. Tetanus neurotoxin-insensitive vesicle-associated membrane protein localizes to a presynaptic membrane compartment in selected terminal subsets of the rat brain. Neuroscience. 2003; 122:59–75. [PubMed: 14596849]

Nosyreva E, Kavalali ET. Activity-dependent augmentation of spontaneous neurotransmission during endoplasmic reticulum stress. J Neurosci. 2010; 30:7358–7368. [PubMed: 20505103]

Pang ZP, Bacaj T, Yang X, Zhou P, Xu W, Sudhof TC. Doc2 supports spontaneous synaptic transmission by a Ca(2+)-independent mechanism. Neuron. 2011; 70:244–251. [PubMed: 21521611]

Prange O, Murphy TH. Correlation of miniature synaptic activity and evoked release probability in cultures of cortical neurons. J Neurosci. 1999; 19:6427–6438. [PubMed: 10414971]

Pryor PR, Jackson L, Gray SR, Edeling MA, Thompson A, Sanderson CM, Evans PR, Owen DJ, Luzio JP. Molecular basis for the sorting of the SNARE VAMP7 into endocytic clathrin-coated vesicles by the ArfGAP Hrb. Cell. 2008; 134:817–827. [PubMed: 18775314]

Ramirez DM, Kavalali ET. Differential regulation of spontaneous and evoked neurotransmitter release at central synapses. Current opinion in neurobiology. 2011; 21:275–282. [PubMed: 21334193]

Ramirez DMO, Andersson S, Russell DW. Neuronal expression and subcellular localization of cholesterol 24-hydroxylase in the mouse brain. J Comp Neurol. 2008; 507:1676–1693. [PubMed: 18241055]

Rizzoli SO, Bethani I, Zwilling D, Wenzel D, Siddiqui TJ, Brandhorst D, Jahn R. Evidence for early endosome-like fusion of recently endocytosed synaptic vesicles. Traffic (Copenhagen, Denmark). 2006; 7:1163–1176.

Sara Y, Bal M, Adachi M, Monteggia LM, Kavalali ET. Use-dependent AMPA receptor block reveals segregation of spontaneous and evoked glutamatergic neurotransmission. J Neurosci. 2011; 31:5378–5382. [PubMed: 21471372]

Sara Y, Virmani T, Deak F, Liu X, Kavalali ET. An isolated pool of vesicles recycles at rest and drives spontaneous neurotransmission. Neuron. 2005; 45:563–573. [PubMed: 15721242]

Scheuber A, Rudge R, Danglot L, Raposo G, Binz T, Poncer JC, Galli T. Loss of AP-3 function affects spontaneous and evoked release at hippocampal mossy fiber synapses. Proc Natl Acad Sci U S A. 2006; 103:16562–16567. [PubMed: 17056716]

Schoch S, Deak F, Konigstorfer A, Mozhayeva M, Sara Y, Sudhof TC, Kavalali ET. SNARE function analyzed in synaptobrevin/VAMP knockout mice. Science. 2001; 294:1117–1122. [PubMed: 11691998]

Shaner NC, Campbell RE, Steinbach PA, Giepmans BN, Palmer AE, Tsien RY. Improved monomeric red, orange and yellow fluorescent proteins derived from Discosoma sp. red fluorescent protein. Nature biotechnology. 2004; 22:1567–1572.

Sutton MA, Ito HT, Cressy P, Kempf C, Woo JC, Schuman EM. Miniature neurotransmission stabilizes synaptic function via tonic suppression of local dendritic protein synthesis. Cell. 2006; 125:785–799. [PubMed: 16713568]

Sutton MA, Taylor AM, Ito HT, Pham A, Schuman EM. Postsynaptic decoding of neural activity: eEF2 as a biochemical sensor coupling miniature synaptic transmission to local protein synthesis. Neuron. 2007; 55:648–661. [PubMed: 17698016]

Takamori S, Holt M, Stenius K, Lemke EA, Gronborg M, Riedel D, Urlaub H, Schenck S, Brugger B, Ringler P, et al. Molecular anatomy of a trafficking organelle. Cell. 2006; 127:831–846. [PubMed: 17110340]

Tochio H, Tsui MM, Banfield DK, Zhang M. An autoinhibitory mechanism for nonsyntaxin SNARE proteins revealed by the structure of Ykt6p. Science. 2001; 293:698–702. [PubMed: 11474112]

Virmani T, Ertunc M, Sara Y, Mozhayeva M, Kavalali ET. Phorbol esters target the activity-dependent recycling pool and spare spontaneous vesicle recycling. J Neurosci. 2005; 25:10922–10929. [PubMed: 16306405]

Virmani T, Han W, Liu X, Sudhof TC, Kavalali ET. Synaptotagmin 7 splice variants differentially regulate synaptic vesicle recycling. The EMBO journal. 2003; 22:5347–5357. [PubMed: 14532108]

Washbourne P, Thompson PM, Carta M, Costa ET, Mathews JR, Lopez-Bendito G, Molnar Z, Becher MW, Valenzuela CF, Partridge LD, Wilson MC. Genetic ablation of the t-SNARE SNAP-25 distinguishes mechanisms of neuroexocytosis. Nat Neurosci. 2002; 5:19–26. [PubMed: 11753414]

Wienisch M, Klingauf J. Vesicular proteins exocytosed and subsequently retrieved by compensatory endocytosis are nonidentical. Nat Neurosci. 2006; 9:1019–1027. [PubMed: 16845386]

Wilhelm BG, Groemer TW, Rizzoli SO. The same synaptic vesicles drive active and spontaneous release. Nat Neurosci. 2010; 13:1454–1456. [PubMed: 21102450]

Xu J, Pang ZP, Shin OH, Sudhof TC. Synaptotagmin-1 functions as a Ca2+ sensor for spontaneous release. Nat Neurosci. 2009; 12:759–766. [PubMed: 19412166]

Zenisek D. Vesicle association and exocytosis at ribbon and extraribbon sites in retinal bipolar cell presynaptic terminals. Proc Natl Acad Sci U S A. 2008; 105:4922–4927. [PubMed: 18339810]

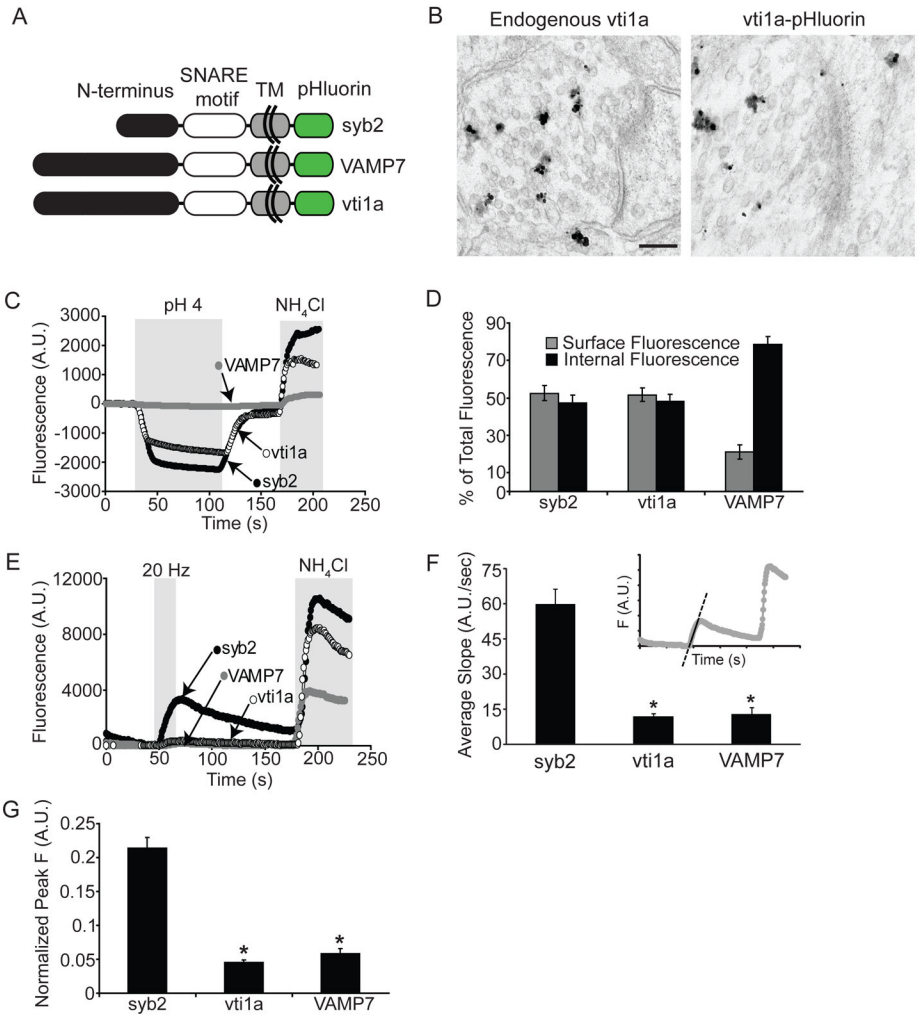

Figure 1. Subcellular localization and trafficking behavior of pHluorin-tagged syb2, vti1a, and VAMP7

(A) Diagram of pHluorin-SNARE fusion proteins used in these experiments.

(B) Representative electron micrographs of neurons immunostained with anti-vti1a antibodies to detect endogenous vti1a or anti-GFP antibodies to detect vti1a-pHluorin. Both native vti1a and vti1a-pHluorin are localized to presynaptic vesicles. Scale bar = 200 nm, applies to both images.

(C) Bath application of acidified (pH 4) and NH_4Cl-containing external solutions onto neurons expressing the indicated pHluorin-tagged constructs to assess surface versus intracellular pools of vti1a, VAMP7 and syb2. Averaged time courses from representative experiments are shown.

(D) Average fluorescence signal localized to the surface or internal compartments for each protein from multiple experiments (n=575 boutons from 10 coverslips for syb2, 468 boutons from 9 coverslips for vti1a, and 112 boutons from 8 coverslips for VAMP7). Error bars in this and in all other figures indicate SEM. Only fluorescent puncta associated with presynaptic boutons were included in the analyses. Syb2 is equally distributed between the surface and internal compartments. Vti1a has a similar distribution, whereas VAMP7 is predominantly localized to internal acidic compartments.

(E) Stimulation at 20 Hz for 20 s produces robust increases in syb2-pHluorin fluorescence due to SV exocytosis, followed by a slow decrease after stimulation due to SV recycling and

re-acidification. Vti1a- and VAMP7-pHluorin show little fluorescence increase during stimulation. Representative time course data from single experiments are shown.
(F) Comprehensive analysis from multiple experiments (n=1417 boutons from 21 coverslips for syb2, 1214 boutons from 21 coverslips for vti1a, and 488 boutons from 10 coverslips for VAMP7) of the rates of the fluorescence increase during 20 Hz stimulation. The inset depicts where the slope values were taken. The differences between syb2 and VAMP7 or vti1a average rising slopes are significant ($p<0.00006$).
(G) Comprehensive analysis from the same experiments as in (E) of peak fluorescence generated during 20 Hz stimulation normalized to the peak fluorescence generated after NH_4Cl treatment. The differences between syb2 and VAMP7 or vti1a average peak values are significant ($p<0.00001$).

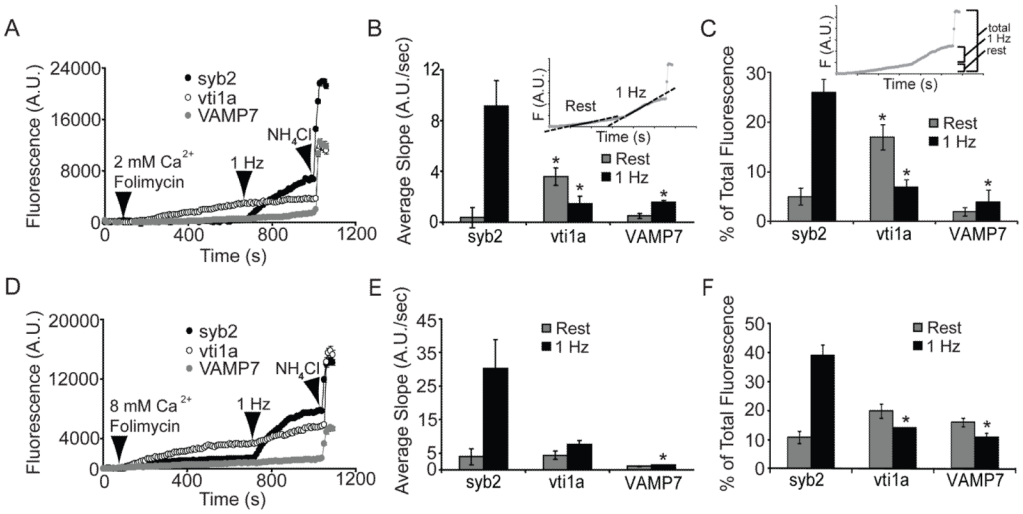

Figure 2. Vti1a is specifically trafficked at rest

(A) Neurons expressing syb2-, vti1a-, or VAMP7-pHluorin were imaged in the presence of 2 mM $CaCl_2$ and 80 nM folimycin at rest for 10 min., followed by field stimulation at 1 Hz for 5 min. Vti1a-pHluorin shows a marked increase in fluorescence at rest over time, whereas syb2 and VAMP7 fluorescence increase only minimally. Only syb2 fluorescence increases at a fast rate upon stimulation, whereas vti1a fluorescence did not increase further with stimulation, suggesting this protein may be specifically involved in spontaneous release. The rate of VAMP7-pHluorin fluorescence increase was slightly faster during 1 Hz stimulation than at rest. Representative time course data from single experiments are shown.

(B) Average data from multiple experiments (n=342 boutons from 6 coverslips for syb2, 265 boutons from 5 coverslips for vti1a, and 128 boutons from 3 coverslips for VAMP7) in which the slope of the fluorescence increase was measured at rest and during stimulation. The inset illustrates where the slope values were taken. The slope value for vti1a fluorescence increase at rest is significantly different than that of syb2 ($p=0.01$). The slope values for vti1a- and VAMP7-pHluorin during 1 Hz stimulation are significantly different than that of syb2 ($p=0.008$ and 0.03, respectively).

(C) Average data from multiple experiments as in (B) showing the percent of total fluorescence changes seen during spontaneous or evoked transmission for syb2-, vti1a-, and VAMP7-pHluorin. The inset depicts how the changes in fluorescence were calculated. The increased fluorescence seen during evoked stimulation was significantly smaller for vti1a and VAMP7 compared to syb2 ($p<0.001$). The increased fluorescence due to spontaneous vesicle trafficking was significantly larger for vti1a compared to syb2 ($p=0.004$).

(D) The experiment shown in Figure 2A was repeated in the presence of 8 mM $CaCl_2$. Increased rates of spontaneous trafficking are seen with all three constructs relative to 2 mM $CaCl_2$, but 1 Hz stimulation cannot induce fusion of the majority of vesicles containing vti1a- and VAMP7-pHluorin even in the presence of increased extracellular Ca^{2+}. The rate of syb2-pHluorin fluorescence increase during stimulation is increased in the presence of 8 mM Ca^{2+} compared to 2 mM Ca^{2+} as expected. Representative time course data from single experiments are shown.

(E) Average data from multiple experiments (n=305 boutons from 4 coverslips for syb2, 125 boutons from 3 coverslips for vti1a, and 105 boutons from 3 coverslips for VAMP7) in which the slope of the fluorescence increase was measured during spontaneous or evoked transmission. The slope value for vti1a fluorescence increase during 1 Hz stimulation shows a trend towards a statistically significant difference from that of syb2 ($p=0.06$). The slope

value for VAMP7-pHluorin during 1 Hz stimulation is significantly different than that of syb2 ($p=0.03$).

(F) Average data from multiple experiments as in (D) showing the percent of total fluorescence changes seen during spontaneous or evoked transmission for syb2-, vti1a-, and VAMP7-pHluorin. The change in fluorescence of vti1a at rest shows a trend towards a statistically significant difference from that of syb2 ($p=0.07$). The increased fluorescence seen during evoked stimulation was significantly smaller for vti1a and VAMP7 compared to syb2 ($p<0.01$).

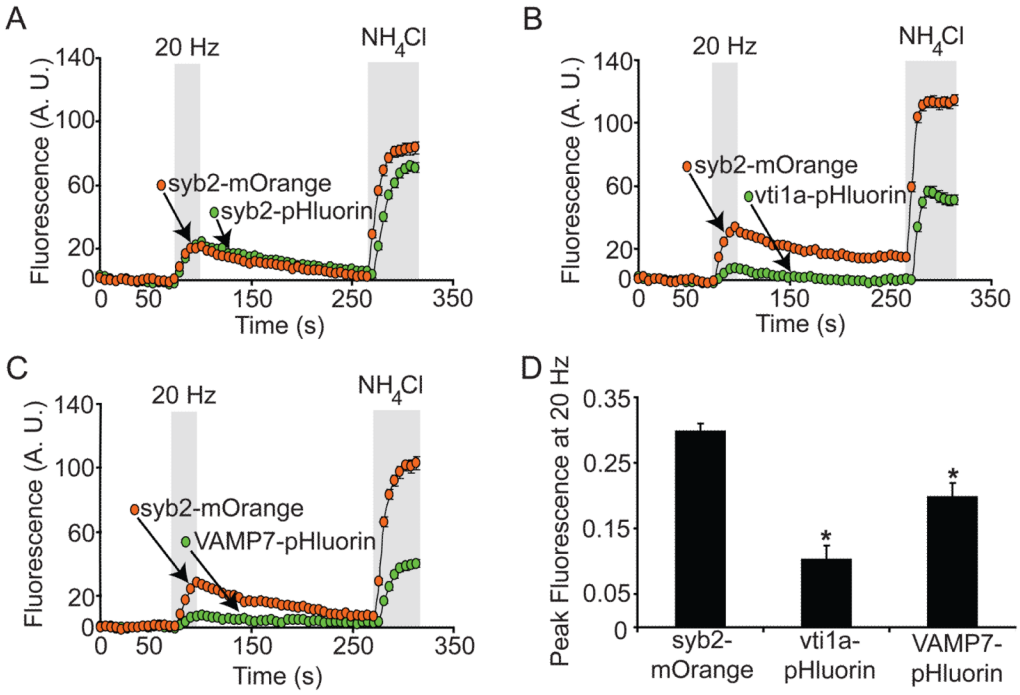

Figure 3. Vti1a and VAMP7 are not efficiently trafficked during stimulation, and are present in the same boutons as syb2

(A) Neurons co-expressing syb2-mOrange and either vti1a- or VAMP7-pHluorin were subjected to field stimulation at 20 Hz frequency for 20 s. Both syb2-mOrange and syb2-pHluorin show increased fluorescence during stimulation due to SV exocytosis, followed by a slow decrease after stimulation due to SV recycling and re-acidification. Representative time course data from single experiments are shown in panels A–C.

(B) Vti1a-pHluorin shows limited fluorescence increase during stimulation, although the syb2-mOrange signal present in the same boutons exhibits a robust increase.

(C) Similar to vti1a-pHluorin, VAMP7-pHluorin fluorescence increases little during stimulation whereas syb2-mOrange present in the same boutons shows a typical response. Syb2-mOrange and syb2-, vti1a-, and VAMP7-pHluorin all show increased fluorescence following NH_4Cl treatment, indicating these proteins are expressed in presumptive SVs.

(D) Comprehensive analysis from multiple experiments (n=425 boutons from 14 coverslips for syb2-mOrange, 105 boutons from 4 coverslips for vti1a-pHluorin, and 60 boutons from 2 coverslips for VAMP7-pHluorin) of peak fluorescence generated during 20 Hz stimulation normalized to the peak fluorescence generated after NH_4Cl treatment. Vti1a-pHluorin exhibits approximately 30% of the fluorescence increase seen with syb2-mOrange, whereas VAMP7-pHluorin shows a more robust increase, though modest relative to syb2-mOrange. The differences between syb2-mOrange and vti1a or VAMP7 average peak values are significant (p=0.000005 for vti1a, p=0.02 for VAMP7).

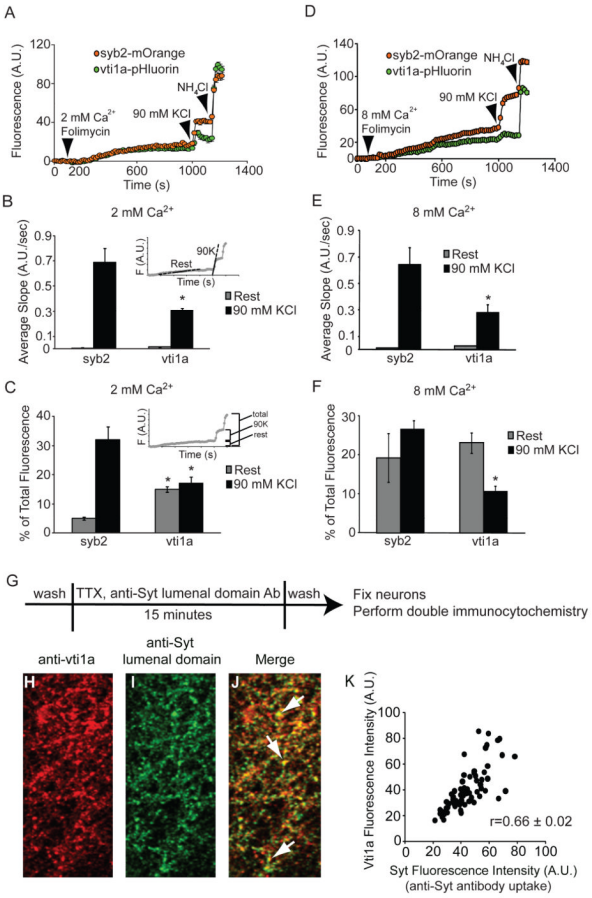

Figure 4. Dual-color imaging confirms selective trafficking of vti1a at rest

(A) Neurons co-expressing vti1a-pHluorin and syb2-mOrange were imaged in the presence of 2 mM $CaCl_2$ and folimycin at rest, followed by chemical stimulation with 90 mM KCl and NH_4Cl treatment. Both vti1a-pHluorin and syb2-mOrange are trafficked at rest, but only syb2-mOrange is substantially mobilized during 90 mM KCl stimulation. Representative time course data from a single experiment is shown.

(B) Comprehensive analysis from multiple experiments (n=40 boutons from 2 coverslips for syb2-pHluorin and 89 boutons from 3 coverslips for vti1a-pHluorin) of the slope values calculated for fluorescence increases at rest and during 90 mM KCl stimulation in 2 mM $CaCl_2$. The inset illustrates where the slope values were taken. Vti1a exhibits significantly less trafficking during stimulation than syb2 (p=0.02).

(C) Comprehensive analysis from the same data presented in (B) of the percent of total fluorescence changes seen at rest or during 90 mM K+ stimulation for syb2- and vti1a-pHluorin. The inset depicts how the changes in fluorescence were calculated. The increased fluorescence seen during 90 mM K+ stimulation was significantly smaller for vti1a compared to syb2 (p=0.05), whereas vti1a exhibited a significant increase in fluorescence at rest relative to syb2 (p=0.003).

(D) As in (A), neurons co-expressing vti1a-pHluorin and syb2-mOrange were imaged in the presence of 8 mM $CaCl_2$ and folimycin at rest, followed by chemical stimulation with 90 mM KCl and NH_4Cl treatment to estimate total protein expression. Both Syb2-mOrange and vti1a-pHluorin are trafficked spontaneously, but only syb2 exhibits substantial trafficking during stimulation in the presence of elevated extracellular Ca^{2+}.

(E) Comprehensive analysis from multiple experiments (n=315 boutons from 6 coverslips for syb2-pHGFP and 700 boutons from 8 coverslips for vti1a-pHluorin) of the rates of fluorescence increases at rest and during 90 mM KCl stimulation in the presence of elevated extracellular Ca^{2+}. The inset illustrates where the slope values were taken. Vti1a exhibits significantly less trafficking during evoked stimulation than syb2 ($p<0.02$).
(F) Comprehensive analysis from the same data presented in (E) of the percent of total fluorescence changes seen at rest or during chemical stimulation for syb2- and vti1a-pHluorin. The inset depicts how the changes in fluorescence were calculated. The increased fluorescence seen during 90 mM KCl stimulation was significantly smaller for vti1a compared to syb2 ($p<0.01$).
(G) Experimental strategy designed to localize endogenous vti1a and spontaneously recycling boutons using antibodies against the vti1a and the lumenal domain of synaptotagmin-1 (syt1).
(H–J) Representative confocal images of neurons immunostained with antibodies against vti1a (shown in red) and the lumenal domain of syt1 (shown in green) according to the experimental strategy shown in (G). Vti1a colocalizes with spontaneously recycling vesicles labeled by uptake of antibodies directed against the lumenal domain of syt1, as shown by white arrows in the merged image.
(K) Intensity plot of the merged image shown in (J). The mean Pearson correlation of the cumulative results for colocalization for vti1a and syt1 from multiple images (n=14 images from two cultures) is indicated on the panel.

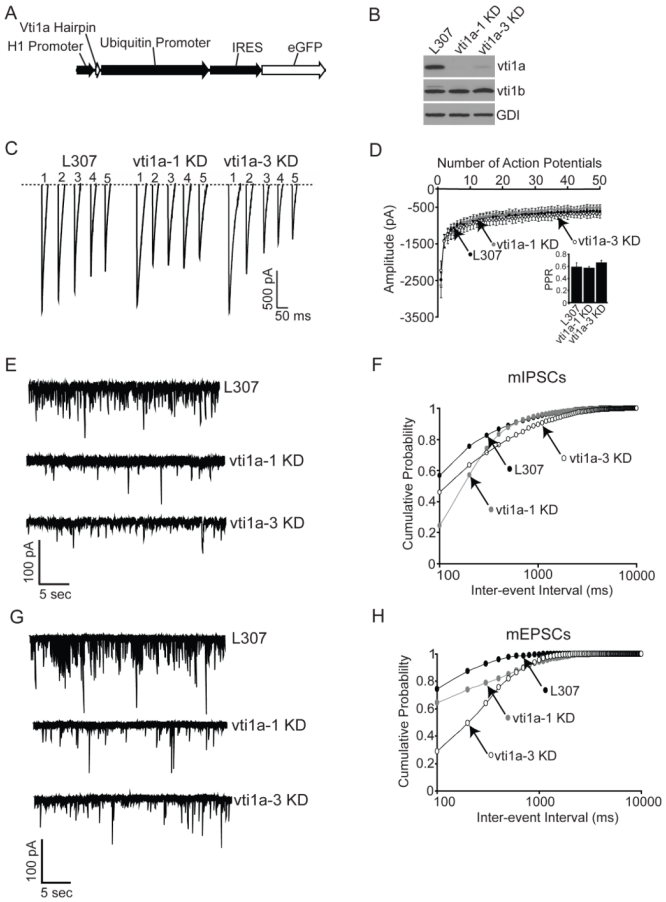

Figure 5. Knockdown of vti1a produces a selective deficit in spontaneous transmission

(A) Schematic diagram of constructs used to produce shRNA directed against vti1a.

(B) Western blot showing the effect of two different knockdown constructs, vi1a-1 KD and vi1a-3 KD, on vti1a, vti1b, and Rab GDP dissociation inhibitor (GDI) expression. Both constructs reduce vti1a expression substantially compared to neurons infected with the empty vector, L307. No changes in the related protein vti1b are evident. GDI was used as a loading control.

(C) Representative traces of the first five IPSC responses in a train of 50 APs given at 10 Hz to neurons infected with the L307 empty vector, vi1a-1 KD or vi1a-3 KD.

(D) Comprehensive analysis of IPSC amplitudes from multiple experiments (n=15 for L307, 21 for vti1a-1 KD, and 19 for vti1a-3 KD). Inset shows average paired pulse ratios from the same recordings. No significant differences were seen in IPSC amplitude or paired pulse ratio between L307- and vi1a-1 KD- or vi1a-3 KD-infected neurons.

(E) Representative mIPSC traces from neurons infected with L307, vi1a-1 KD or vi1a-3 KD.

(F) Cumulative probability histograms of mIPSC inter-event intervals from multiple experiments (n=13 for L307, 17 for vti1a-1 KD, and 11 for vti1a-3 KD). Both vti1a-1 KD and vti1a-3 KD significantly decrease high-frequency events compared to L307-infected neurons (Kolmogorov-Smirnov (K–S) test, vti1a-1 KD p=0.0001, vti1a-3 KD p=0.0001).

(G) Representative mEPSC traces from neurons infected with L307, vti1a-1 KD or vti1a-3 KD.

(H) Cumulative probability histograms of mEPSC inter-event intervals from multiple experiments (n=3 for L307, 6 for vti1a-1 KD, and 3 for vti1a-3 KD). Both vti1a-1 KD and

vti1a-3 KD significantly decrease high-frequency events compared to L307-infected neurons (K–S test, vti1a-1 KD p=0.0001, vti1a-3 KD p=0.0001.).

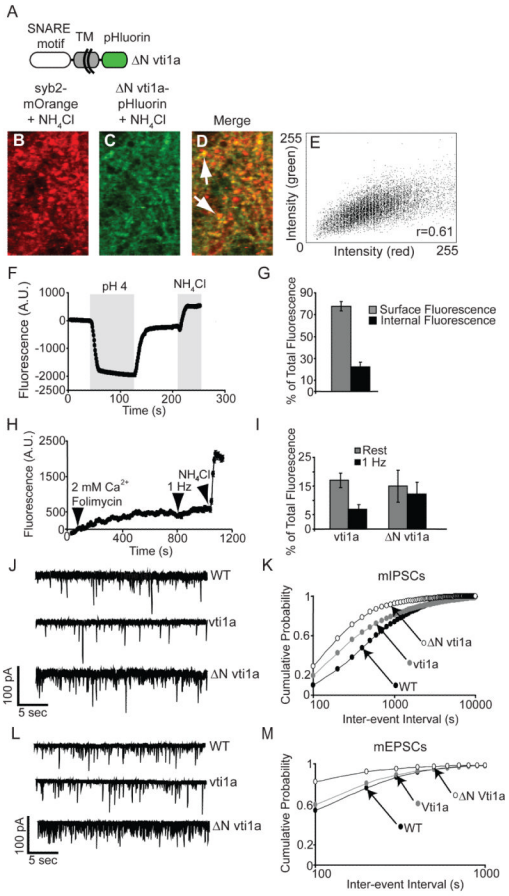

Figure 6. Expression of ΔN vti1a-pHluorin in wild-type neurons increases miniature event frequency

(A) Schematic diagram of ΔN vti1a-pHluorin.

(B–D) Representative confocal images taken after NH_4Cl application of neurons co-expressing ΔN vti1a-pHluorin with syb2-mOrange.

(E) Intensity plot of the image shown in (D) and the calculated Pearson correlation coefficient of colocalization for ΔN vti1a-pHluorin and syb2-mOrange.

(F) Bath application of acidified (pH 4) and NH_4Cl-containing external solutions to assess relative surface expression of ΔN vti1a-pHluorin. An averaged time course from a representative experiment is shown.

(G) Average data from multiple experiments are shown (n=160 boutons from 4 coverslips). ΔN vti1a-pHluorin is predominantly localized to the neuronal surface.

(H) ΔN vti1a-pHluorin trafficking was measured at rest and during 1 Hz stimulation in the presence of folimycin and 2 mM $CaCl_2$ as in Figure 2. Some ΔN vti1a-pHluorin is mobilized at rest and the rate of this fluorescence increase does not increase during 1 Hz stimulation, similar to the behavior of full-length vi1a (Figure 2). Representative time course data from a single experiment is shown.

(I) Combined data from multiple experiments measuring spontaneous and evoked trafficking of ΔN vi1a-pHluorin are shown (n=85 boutons from 3 coverslips). Results are expressed as a percentage of total internal fluorescence as judged by NH_4Cl treatment. ΔN vi1a- and vi1a-pHluorin exhibit similar trafficking behaviors at rest and during 1 Hz stimulation. Vti1a-pHluorin cumulative data are reproduced from Figure 2.

(J) Representative mIPSC traces from uninfected neurons and neurons expressing full-length vi1a-pHluorin or the truncation mutant ΔN vti1a-pHluorin.

(K) Cumulative probability histograms of mIPSC inter-event intervals from multiple experiments (n=17 for wild-type, 18 for vti1a-pHluorin, and 6 for ΔN vti1a-pHluorin). Both vti1a-pHluorin and ΔN vti1a-pHluorin significantly increased mIPSC frequency compared to uninfected neurons (K–S test, vti1a-pHluorin p=0.0001, ΔN vti1a-pHluorin p=0.0001).
(L) Representative mEPSC traces from uninfected neurons and neurons expressing full-length vti1a-pHluorin or the truncation mutant ΔN vti1a-pHluorin.
(M) Cumulative probability histograms of mEPSC inter-event intervals from multiple experiments (n=8 for wild-type, 8 for vti1a-pHluorin, and 7 for ΔN vti1a-pHluorin). Both vti1a-pHluorin and ΔN vti1a-pHluorin significantly increased mEPSC frequency compared to uninfected neurons (K–S test, vti1a-pHluorin p=0.0001, ΔN vti1a-pHluorin p=0.0001).

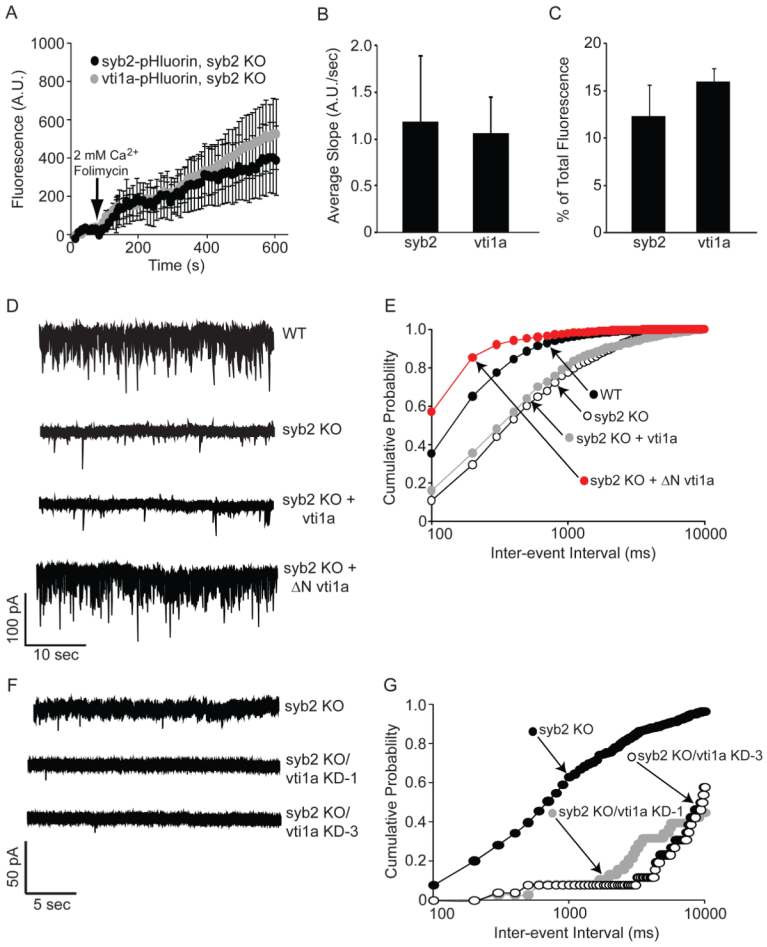

Figure 7. Spontaneous trafficking of vti1a is syb2-independent

(A) Syb2 KO neurons expressing syb2- or vti1a-pHluorin were imaged in the presence of 2 mM $CaCl_2$ and 80 nM folimycin at rest for 10 min. and fluorescence changes were monitored. Syb2- and vti1a-pHluorin show similar increases in fluorescence at rest, indicating that vti1a does not require syb2 for its spontaneous trafficking.

(B) Average data from multiple experiments (n=211 boutons from 4 coverslips for syb2 and 323 boutons from 5 coverslips for vti1a) in which the slope of the fluorescence increase for syb2- and vti1a-pHluorin was measured during spontaneous transmission in syb2 KO neurons. The slope values for syb2 and vti1a fluorescence increases at rest are not significantly different.

(C) Average data from multiple experiments as in (B) showing the percent of total fluorescence changes seen during spontaneous activity in syb2 KO neurons expressing syb2- or vti1a-pHluorin. Fluorescence increased at rest for both syb2- and vti1a-pHluorin, and these changes in fluorescence were not significantly different.

(D) Representative mIPSC traces from uninfected wild-type or syb2 KO neurons or syb2 knockout neurons expressing vti1a- or ΔN vti1a-pHluorin.

(E) Cumulative probability histograms of mIPSC inter-event intervals from multiple experiments (n=8 for wild-type, 8 for syb2 KO, 10 for syb2 KO expressing vti1a-pHluorin, and 3 for syb2 KO expressing ΔN vti1a-pHluorin). Vti1a-pHluorin expression did not affect mIPSC frequency compared to uninfected syb2 KO neurons, whereas ΔN vti1a-pHluorin significantly increased mIPSC frequency (K–S test compared to wild-type neurons, p=0.0001 for syb2 KO, vti1a-infected syb2 KO, and ΔN vti1a-infected syb2 KO. K–S test

compared to syb2 KO neurons, p=1 for vti1a-infected syb2 KO, p=0.0001 for ΔN vti1a-infected syb2 KO).

(F) Representative mIPSC traces from uninfected syb2 KO neurons or syb2 KO neurons infected with vti1a-1 KD or vti1a-3 KD.

(G) Cumulative probability histograms of mIPSC inter-event intervals from multiple experiments (n= 5 recordings for syb2 KO, 5 for syb2 KO/vti1a-1 KD, and 3 for syb2 KO/vti1a-3 KD). Vti1a knockdown in the absence of syb2 using either construct significantly decreased mIPSC frequency (K–S test compared to uninfected syb2 KO neurons, p=0.0001 for vti1a-1 KD and vti1a-3 KD).